

Characterization of a marine intrusion using electrical sounding and seismic refraction: case of the the Oued Nador plain (Tipaza, Algeria)

Mohamed Amine Bechkit (✉ mohamed-amine.bechkit@hotmail.fr)

University of Sciences and Technology Houari Boumediene: Universite des Sciences et de la Technologie Houari Boumediene

Seid Bourouis

CRAAG: Centre de Recherche en Astronomie Astrophysique et Geophysique

Fayçal Chafiheddine Mouhoub

CRAAG: Centre de Recherche en Astronomie Astrophysique et Geophysique

Moussa Aichaoui

CRAAG: Centre de Recherche en Astronomie Astrophysique et Geophysique

Khiereddine Arrache

CRAAG: Centre de Recherche en Astronomie Astrophysique et Geophysique

Research Article

Keywords: marine intrusion, salt water, electrical sounding, seismic refraction

Posted Date: March 23rd, 2022

DOI: <https://doi.org/10.21203/rs.3.rs-1327688/v1>

License: © ⓘ This work is licensed under a Creative Commons Attribution 4.0 International License. [Read Full License](#)

Abstract

The present study aims to characterize, by geophysical methods (electrical sounding and seismic refraction), the downstream part of the Oued Nador alluvial layer or deposits (Tipaza, Algeria) and the morphology of its bedrock to better locate the freshwater-saltwater limit. This will allow to better understand the marine intrusion.

Indeed, the aquifer is defined by a clay and marl substratum of middle to lower Pliocene Piacenzian age rich in recent Neogene and Quaternary filling (Quaternary alluvium composed of sand, gravel and pebbles).

During Spring of 2015, 2016, and 2017 three electrical surveys were conducted. The results indicate that the origin of the salinity is due to progressive marine intrusion inside the aquifer (Bechkit et al, 2017; Bechkit et al, 2018a; Bechkit et al, 2018b). However the presence of clay makes the contrast between the saltwater and the clays less important so that it is difficult to distinguish electrically the two mediums. In May 2018, we combined both electrical survey and a refraction seismic acquisition on the area of study. This work was carried out in order to separate, through the ranges of wave propagation velocity, the saltwater formations from the clay ones. The presence at a certain distance from the coast of an elevation of the clay bedrock has an advantage. Indeed, it acts as a natural barrier against any intrusion on a large scale of saltwater at depth. The study carried out in this context showed that the combination of two geophysical methods is very useful in environmental study for the evaluation of the salt water intrusion in an alluvial ground in the presence of clay formations.

Introduction

Groundwater resources have become a national concern due to several factors, particularly intensive exploitation generated by population growth and agricultural and industrial development. In 2021, about 90% of Algerians live near the Mediterranean coast. As a result, a large part of Algeria's population is dependent on coastal water resources and for the majority on groundwater resources. In addition, high water demands occur during the summer season, when groundwater levels are at their lowest (Comte, 2008; Moulla, 2013; Cocheril, 2019; Inim, 2020).

Algeria's annual water needs by 2030 will reach about 13 billion m³. Currently, about 20% of the needs are provided by groundwater. The level of groundwater renewal is dependent on meteorological conditions, such as rainfall, this later is rare which increase our vulnerability to climate change (Comte, 2008; Priju, 2018). A simple rise in sea level directly affects the water quality of coastal aquifers and accelerates the process of marine intrusion. Water quality degradation is generally expressed as contamination due to salinization of freshwater by Salt water (Bouderbala and Remini, 2014; Senthilkumar, 2019).

The aquifer of Nador (Tipasa, Algeria), located on the Mediterranean coast under a semi-arid climate. The geographical situation of the aquifer and the excessive water pumping, can create an imbalance between the two liquids and favor the migration of seawater inside the aquifer. This is due to a decrease in the piezometric level of the fresh water. According to the principle of density, the seawater below the fresh water extends into the aquifer, forming the salt wedge. The extent of the seawater inside the aquifer causes the salinization of the exploitation wells. This induces their closure and abandonment, creating a deficit in fresh water.

Hydrogeological studies, conducted by Taibi and Hamadache in 1992, Bouderbala (2015a) and Bouderbala et al. (2016a), seem to indicate that in the Oued Nador aquifer the limit of the salt wedge reached a distance of 1700 m far from the coast. The electrical surveys, we carried out during May of 2015, 2016 and 2017, seems to indicate that the origin of the salinity is due to the marine intrusion far inland inside the aquifer.

To avoid the pollution of the freshwater table by salt water requires: a) a better knowledge of the physics of the recharge of the aquifer by freshwater, b) an powerful and robust management and c) a protection of the freshwater resource.

In this article, we will focus on the downstream part of the plain located in the Oued Nador area, Tipaza (Algeria). The objective of this work is to detect the current position of the salt wedge and to estimate its spatio-temporal evolution. To achieve this objective, we have chosen to use jointly electrical soundings and seismic refraction. These two geophysical methods are complementary: the electrical survey is based on the measurement of resistivity, and the seismic refraction measures the velocity of propagation of waves in the medium.

The large resistivity contrast between saturated saltwater and saturated freshwater- formations has been used by many researchers to study saltwater intrusion in coastal areas (Choudhury, 2001; Batayneh, 2006; Sathish et al., 2011; Oyeyemi et al., 2015; Kumar et al., 2016; Adeyemo, 2017; Yusuf et al., 2019; ...). Only, the presence of clay formations makes the resistivity contrast, between clays and saltwater saturated formations, lower. The resistivities of conductive and saltwater saturated aquifer formations are generally between 1 and 10 ohm.meter (Demirci, 2020). It is the same resistivity range, (between 7 and 10 ohm.meter), that characterize the marls and clays of the Nador aquifer (Bouderbala, 2015b; Bechkit et al., 2017, 2018a and 2018b).

The superposition of several effects such as: a) lower contrast in terms of electrical resistivity between salt water and clays, b) presence of barriers (elevation of the bedrock) of clay and c) up-welling towards the surface of the soil, in the form of a salt dome and d) up-welling in the form of an uplift of the interface freshwater - saltwater, makes the interpretation more delicate and make difficult the determination of the interface of

separation freshwater - saltwater. In addition, the effect of soil moisture can influence the determination of the position of the freshwater-saltwater interface. The electrical resistivity depends on the state of moisture of the soil, for this we have established a water balance (Tab. 1), this is true in the case of a rainy episode that follows a period of drought, because there is also the effect of dissolution by rainfall, dry salts located near the surface of the soil in the unsaturated zone. The use of seismic refraction allows to separate, through the velocity ranges, the salt water formations from the clay formations and to specify the structure of the formations.

Table 1
Hydric balance (September 2017 - August 2018).

Sep 2017 - Aug 2018	Sep	Oct	Nov	Dec	Jan	Feb	Mar	Apr	May	Jun	Jul	Aug	Sum
P (mm)	14.00	33.00	68.00	78.00	39.00	99.00	121.00	160.00	67.00	66.00	2.00	0.00	747.00
T (°C)	26.00	22.00	16.00	12.00	13.00	11.00	14.00	18.00	20.00	26.00	31.00	30.00	
PET (mm)	135.41	100.71	56.94	37.04	42.96	33.54	56.47	86.02	109.81	158.80	206.70	184.65	1209.04
EUR (mm)	0.00	0.00	11.06	52.02	48.06	100.00	100.00	100.00	57.19	0.00	0.00	0.00	
RET (mm)	14.00	33.00	56.94	37.04	42.96	33.54	56.47	86.02	109.81	123.19	2.00	0.00	594.96
Excess (mm)	0.00	0.00	0.00	0.00	0.00	13.52	64.53	73.98	0.00	0.00	0.00	0.00	152.04
AD (mm)	121.41	67.71	0.00	0.00	0.00	0.00	0.00	0.00	0.00	35.61	204.70	184.65	614.08

In order to delineate the freshwater-saltwater interface, to determine the nature and morphology of the geological formations and to validate the hypothesis of the local elevation of the bedrock, acting as a natural barrier and preventing any marine intrusion, we have completed, in 2018, the electrical measurements by a seismic refraction survey. These measurements enabled to distinguish clays from salt water and to determine the diopeter inclination within the prospected depth range.

Indeed, the simultaneous interpretation of the results of the electrical soundings, the seismic profiles and the hydrostatic approach allow to significantly reduce the uncertainties related to each of these methods independently used.

Geographical Framework

The city of Tipaza (Algeria) is located on the Mediterranean coast, 75 km west of Algiers (Fig. 1a). Its domestic water supply as well as for agricultural purposes rely essentially on the exploitation of groundwater from the Oued Nador aquifer. Located west of Tipaza, the Oued Nador groundwater is integrated in a coastal geological unit, formed by sand-clay soils of the Plio-Quaternary units, which is called the Sahel of Algiers. It is limited to the north by the Mediterranean Sea, to the south and east by the slopes of the Sahel and to the west by the Chenoua massif (Fig. 1b).

Geological Setting

The plain of Oued Nador belongs to the Western Mitidja basin (Fig. 1b), it is according to (Bouderbala, 2015) a syncline with Plio-quaternary sandy-clay filling (Fig. 2). It is a valley that follows a synclinal feature, with sandy-clay filling of plio-quaternary age, oriented NNE-SSW, whose main axis is occupied by the Oued Nador, which gave its name to the plain. The Pliocene formations are composed of two layers: a) the Piacenzian : (lower Pliocene) form a thick and uniform series of grey and blue marls sometimes sandy which are well presented in the East of Oued Nador, b) the Astien: include the level with glauconite and the molasse astian. The quaternary series: are composed by marine deposits on the sandstone-limestone astian. They are formed of pebbled sands, conglomerates and micro conglomerates with calcareous cement, topped by alluvial deposits. Glangeaud (1932), classifies in the lower Pliocene: the blue marls of the piacenzian, the level with glauconia and the yellow sandstone marls of the base of the Astien, and in the upper astian or lower Calabrian the red sandstones and the Puddingstone. Ayme et al. (1954) and Hachemi (2015), classified in the Lower Pliocene (Piacenzian) the blue marls and in the Upper Pliocene (Astian), the glauconite level and the sandstone-limestone deposits and sandstone marls located above the previous level. For this author, the conglomerate below the lower Pliocene marks the boundary between the Miocene and the Pliocene, belonging either to the late Miocene or the early Pliocene.

Figure 3a shows the lithological series from borehole F3, 110 m deep (Taibi and Hamadache, 1992), located about 500 m from our study area. The results obtained from the test hole are shown in Figure 3b (Taibi and Hamadache, 1992). Beyond 48 m, the series is clearly clayey with sandy passages. It should be noted that the Oued Nador plain has undergone the same tectonic and paleogeographic evolution as that which affected the Mitidja basin.

Hydrodynamics And Hydrochemistry

The piezometric map and the litho-stratigraphic log (drilling F3) allowed Taibi and Hamadach (1992) to highlight :

- an aquifer consisting mainly of gravel, sand and a calcareous-sandstone series.

- a penetration of water from North to South along the coast, which causes a probable contamination (piezometric levels below sea level) by marine waters. In addition, these authors show that the sodium chloride chemical elements are dominant (75%) in the Oued Nador region, hence the risk of soil alkalinization and high salinity for certain crops. The maps of the concentration of the chemical elements (Cl^- , Na^+ , Mg^{++} et Ca^{++}), and the characteristic ratios reported by ($r.\text{Cl}/\text{Hco}_3$ et $r.\text{Mg}/\text{Ca}$) (Taibi and Hamadach, 1992) and those of Bouderbala et al. (2016b) show the presence of high concentration zones in the wells close to the coast. These anomalies are probably related to the influence of the salt waters (Taibi and Hamadach, 1992 ; Bouderbala et al. 2016c).

Hydro-climatology

The Nador plain is an important hydrogeological unit. It is entirely included in the watershed noted "Algiers Coastal Basin". The tributaries are in their majority temporary wadis. To determine the effect of overexploitation of water, the groundwater recharge and the position of the freshwater - saltwater interface, a water balance is carried out for the period from September 2017 to August 2018. During this period, the recorded annual precipitation was about 750 mm and the average monthly temperatures range from 11°C to 31°C (Fig. 4).

Figure 4 shows the basic data for determining the water balance according to the Thornthwaite (1948) method. There are several methods to calculate the water balance, due to lack of data, we have chosen the Thornthwaite (1948) method. This method is based on the average monthly precipitation and temperature; it allows to estimate the potential evapotranspiration (PET), the real evapotranspiration (RET), the surplus and agricultural deficit (AD). The results of the water balance are given in Table 1. We observe that the real evapotranspiration is 594.96 mm or 79.64% of the precipitation. From November to December and from February to April, the precipitation is higher than the potential evapotranspiration which is 1209.04 mm. We note that April (the month before our electrical and seismic surveys) is an exceptional month of 2018, with 160 mm of precipitation.

The easily usable reserve (EUR) reaches its maximum between February and April, i.e. 100 mm, yielding a reservoir storage surplus on the order of 152 mm. A decrease in the EUR is observed at the beginning of May until it becomes zero in June. The agricultural deficit is 614.08 mm. This is explained by the existence of two deficit periods: the first extends from September to October and the second begins in June and continues until August.

According to the classification of climates of Köppen, the area of Tipaza is located in the CS zone (characterized by a warm temperate climate with a dry summer (Hufty, 2001)). This zone defines the climate as being of the Mediterranean type with hot and arid summer, while the rest of the year is rainy and less hot (Boukhelifa, 2014).

Data Acquisition And Processing

In this study, we conducted electrical soundings and seismic refraction profiles. The Schlumberger device, which we used, is sensitive to vertical variations, therefore it is suitable for the study of marine intrusions (Nowroozi et al. 1999). During May 2018 we performed seven electrical soundings, using an IRIS-SYSCAL R1 resistivity meter (Fig. 1c). The AB lines are oriented NW-SE with lengths between 280 m and 680 m. During the same period, we made two seismic refraction profiles, with a 24 channel STRATAVIEW seismograph. The length of the first is 205 m with an overlap and 133 m for the second. The measurements were made with a regular sampling of (6 meters) between two geophones, a direct shot (DS), a center shot (CS) and a reverse shot (RS).

Inversion of the electric sounding data with IPI2Win software (Bobachev, 1994), allowed us to approximate the electrical structure of the field. For simultaneous interpretation of the seven electrical soundings, carried out in May 2018, we used the results of the F3 lithostratigraphic log and the standard electrical sounding (Fig. 1c, Fig. 3b) (Taibi and Hamadache, 1992). Figure 5 shows the pseudosection of the apparent resistivity and the actual values of the geoelectric section. Figure 6a represents a schematic section realized with the IPIres3 software (Bobachev, 1994). It shows the geometric distribution of the geo-electric section, the real values of the resistivity on which the freshwater-saltwater separation interface has been superposed, with resistivity values that can reach 50 ohm.meter for freshwater formations and values lower than 10 ohm.meter for formations saturated with saltwater (Kumar, 2020).

The seismic refraction is based on the analysis of compression waves (P) refracted at the top of the layers. It allowed us to determine the velocities and thicknesses of the different layers. Indeed, it allowed us to obtain two hodochrones of the seismic profiles, the seismic profile PS1 which is composed of two overlapping sections of a total length of 205 m and the seismic profile PS2 which has a length of 133 m. The data processing allowed us to obtain a general geoseismic section of the two profiles (Fig. 7). Figure 7 is a seismic tomography section made with SeisImager/2D software (OYO Corporation, 2005). It shows the geometric distribution of the geological formations, including the existence of three layers, with absolute values of propagation velocities ranging from 640 m/s to 2200m/s.

Hydrostatic Approach

The form and thickness of the freshwater-saltwater interface depend on several factors: the variations of the levels of the freshwater (both recharge and exploitation) and the sea level, the difference in density between the two liquids which tends to maintain the saltwater at depth, the molecular diffusion of salt in the freshwater tending to minimize the concentration gradients, the porosity and permeability of the different layers. In our case, we must add the geometry of the aquifer (the morphology of the impermeable clay bedrock at the freshwater-saltwater interface).

Several approaches provide insight into the positioning of this freshwater saltwater interface, whose hydrostatic and hydrodynamic approaches (Hubbert, 1940; Cooper, 1959; Glover, 1959). In this study, in the absence of information on groundwater flow and the freshwater-saltwater mixing zone, we opted for a comparison between the results of the electrical soundings and the hydrostatic approach of Ghygen-Herzbeg (Badon-Ghijben, 1889 and Herzberg, 1901), which determines the theoretical position of the salt wedge from the following relationship:

$$H = \left(\frac{d_s}{d_s - d_d} \right) * h \quad (1)$$

With :

d_s : the density of salt water,

d_d : the density of fresh water,

h: the height of fresh water above sea level at a given point,

H: the height of the interface.

The density of seawater varies with salinity; it is equal to 1025 kg/m³; the density of fresh water is equal to 1000 kg/m³.

For Ghygen-Herzbeg, the contact is assumed to be represented by a sharp interface, and freshwater and saltwater are considered as two non-miscible fluids. This hydrostatic approach gives us the form and theoretical position of the freshwater-saltwater interface. This enabled us to formulate the scenario illustrated in figure 6b.

These different treatments give us to jointly interpret the results of the seismic tomography and the results of the electrical surveys. A comparison with the results of the hydrostatic approach is the equivalent of an external validation.

Results And Interpretations

The presence of low contrast formations (conductive aquifer formations saturated with saltwater and clay formations) complicates the determination of the freshwater-saltwater separation surface.

Interpretation of the inversion results of the electrical soundings, the standard sounding and the litho-stratigraphic log have enabled us to highlight the following formations

- a silty surface formation with a resistivity varying between 15 and 33 ohm.meter,
- a marl-clay formation, rather conductive, with resistivity varying between 10 and 23 ohm.meter,
- a clay formation which acts as a natural barrier against any marine intrusion. We note that it is quite difficult to distinguish electrically this clay formation from the porous saltwater formations,
- a resistive level saturated with fresh water with a resistivity that reaches 50 ohm.meter,
- a level of low resistivity, less than 10 ohm.meter, corresponding to the interface separating the freshwater - saltwater formation,
- in the proximity of the electrical sounding n°7 (se7) the resistivity values locally exceed 100 ohm.meter; this indicates the presence of the pebble and conglomerate formations.

The freshwater-saltwater interface is irregular (Fig. 6a). The depth of the interface is 42 m at the level of se2 sounding and 58 m below se3 sounding. It rises quickly to the surface, at a depth of 12 m and 32 m, in se4 and se5 soundings respectively. The maximum depth is 80 m at the se6 sounding, which is located 460 m from the se2 sounding. It rises back to the surface at the level of sounding se7 at 64 m and at 55 m at the level of se8 sounding.

We observe a rapid rise of the freshwater - saltwater interface between se3 and se4, we suppose that this is caused by: first, the over-exploitation (between se3 and se5) of the water table for agricultural needs, on the other hand, the presence of a conductive formation of low resistivity, different from the saltwater, between se3 and se5 or around the se4 sounding. This conductive formation with low resistivity is a clay barrier. It

acts as a natural barrier against any large-scale intrusion of salt water. It slows down and brakes the extension of the saltwater wedge upstream and enables us to explain the rapid fall of the freshwater-saltwater interface. The rise of the interface between se6 and se8 is mainly due to the over-exploitation of the freshwater for agricultural needs. Indeed, despite the high rainfall of the hydrological year (September 2017 - August 2018) which is 747 mm, this was not enough to reduce the over-exploitation of this groundwater.

The results of the hydrostatic approach (Fig. 6b) show that the freshwater-saltwater interface, obtained by the Ghyben-Herzberg (1901) model, follows the same behavior as the interface obtained from the schematic section. This gait of the interface is consistent with the one obtained with the electrical surveys in May 2018. From the water balance analysis, we observe for the month of May (the period concerned by our electrical and seismic measurements) the following results: precipitation is 67 mm, which is less than the potential evapotranspiration (PET). The latter is equal to the RET which is 109.81 mm. We also observe a decrease in the EUR to 57 mm. The agricultural surplus and deficit are null. From the water balance we were able to point out a possible influence of soil humidity on the quality of our electrical measurements and thus on the determination of the position of the freshwater-saltwater interface. The principal source of difficulty in interpreting the electrical sounding data is the presence of clay. The latter makes the contrast between the salt water formation and the clays lower, this is why we cannot distinguish electrically the two mediums. For this reason, we used seismic refraction.

The results of the two geoseismic sections obtained show three layers:

1- the velocity of the first layer varies between 640 m/s and 840 m/s with a thickness ranging between of 1 m to 3 m. We attribute these velocity to a limonous formation,

2- a second layer with a thickness varying between 6 m and 26 m with a velocity between 1720 m/s and 1820 m/s. These are assigned to humid alluvial formations,

3- the last layer corresponds to a clay formation characterized by high velocities between 2100 m/s and 2200 m/s. The analysis of the two seismic refraction profiles, allowed us to draw up a general geoseismic section of 338 m thickness. This last one highlights : a) the velocities and depths of the different layers, b) the morphology of the layers (inclination of the diopeters) and c) the presence of a rising clay substratum, which has the role of a natural barrier.

The joint interpretation of the two techniques (electrical sounding and seismic refraction) allowed us to propose a characteristic model in agreement with the lithology of the study region.

The electrical method enable us to position in space and time the freshwater-saltwater separation surface, based on the contrast between the resistivity values of the two media. Seismic has completed these results where the contrast is less important. It allowed to remove the ambiguity and to differentiate two media close in terms of resistivity values, namely clays and salt water. This is especially true in the proximity of surveys se3 and se5 (Fig. 6a). Furthermore, we were able to confirm the presence of a rise in the clay substratum (Fig. 7).

Conclusion

This study was carried out for a better understanding of the marine intrusion in a context of clay substratum uplift. The results of the electrical and seismic refraction surveys are in good agreement. Indeed, the electrical soundings allowed us to highlight the two zones of interest to us; the freshwater saturated zone, characterized by a high resistivity and the salt-water saturated zone of low resistivity compared to the freshwater saturated zone. Although there is an ambiguity between the interpretation of low resistivity due to the presence of a rise of the clay substratum and that due to the presence of salt water or a salt dome called cone of rise of the surface separation freshwater - salt water which is due to the over-exploitation of the water table locally. However, this ambiguity has been resolved by the use of seismic refraction. This technique has allowed us to highlight three layers with velocities of about 800 m/s, 1800 m/s and 2200 m/s representing respectively the silts, the wet alluvium and the clays. The morphology of the clay layer confirms the rise of the clay substratum in the area surrounding the se3 and se5 surveys.

Although the depth of the seismic investigation does not exceed 42 m in our case, these two methods were complementary. The seismic survey gave us an idea of the dip of the diopres and the presence and position of the clay layer. A seismic acquisition with a large device is more than necessary to cover the down-stream part of Oued el Naodr plain, a part already prospected by the 7 electric surveys with a length AB between 280 m and 680 m. The objective is to attain the most profound layers, in seismic, to know better the geometry of the substratum clayey. This will permit us to understand the natural barrier role of this clay formation (substratum) that slows down the advancement of the marine intrusion. From the hydric balance analysis, we obtained insight into the soil humidity and its limited influence on the quality of our electrical measurements. The results obtained by the Ghyben-Herzberg (1901) model, follow the same trend as the interface obtained from the schematic section.

Finally, a more and more rational management is most necessary in order to increase and improve the thickness of the freshwater aquifer.

Declarations

Acknowledgements :

This study was conducted with the support of the Houari Boumediene Sciences and Technology University geophysics laboratory and Centre de Recherche en Astronomie Astrophysique et Géophysique (C.R.A.A.G) Alger, Algeria, using an resistivity-meter and seismograph.

Authors Contributions

All authors contributed to the conception and design of the present study. This draft was commented and approved by all the authors.

Funding

This research received no specific grant from any funding agency in the public, commercial, or others."

Availability of Data and Material The information has been obtained through surveys. If necessary, the data could be made available.

Ethics Approval All work is compliance with Ethical Standards.

Consent to Participate Authors consent to their participation in the entire review process.

Consent for Publication Authors allow publication if the research is accepted.

Competing Interests The authors declare that they have no known competing financial interests or personal relationships that could have appeared to influence the work reported in this paper.

References

1. Adeyemo IA, Omosuyi GO, Adelusi AO (2017) Geoelectric soundings for delineation of saline water intrusion into aquifers in part of eastern Dahomey basin, Nigeria. *J Geoscience Environ Prot* 5(3):213–232
2. Ayme A (1954) Etude des terrains néogènes de la cluse du Mazafran (Sahel d'Alger). *Bull. Serv. Carte géol. Algérie, Nouv. Ser., n°1, trav. Coll., Fasc. II: 129-150*
3. Badon-Ghijben W (1889) Nota in verband met de voorgenomen putboring nabij Amsterdam, *Tijdschrift het koninglijk. Instituut voor Ingenieurs, Den Haag, pp 8–22*
4. Batayneh AT (2006) Use of electrical resistivity methods for detecting subsurface fresh and saline water and delineating their interfacial configuration: a case study of the eastern Dead Sea coastal aquifers. *Jordan Hydrog J* 14:1277–1283
5. Bechkit M, Benaissa A, Deghmoum Z, Ouadfeul SA (2017) Salt wedge determination using electrical sounding method in the region of Oued Nador (Tipaza, Algeria). Vienna, Austria. Session G11.1/EMRP4.16/SSS12.25, abstract EGU2017 – 10129
6. Bechkit M, Deghmoum A, Chabour F, Bourouis S (2018a) Rôle d'une barrière naturelle sur l'évolution d'une intrusion marine dans la région d'Oued Nador Tipaza (Algérie). Communication au 7ème Colloque Maghrébin de Géophysique Appliquée CMGA 7 – Algiers
7. Bechkit M, Benaissa A, Deghmoum F (2018b) Rainfall effect on the salt wedge using electrical sounding method in Oued Nador region (Tipaza, Algeria). Communication au 9th International Symposium on Eastern Mediterranean Geology – Antalya, Turkey
8. Bobachev AA (1994) IPI2Win software: http://geophys.geol.msu.ru/rec_labe.htm
9. Bouderbala A, Remini B, Saaed Hamoudi A (2016a) Geoelectrical investigation of sea water intrusion in the coastal aquifer of Nador (Tipaza, Algeria). 3ème colloque international sur la géologie du Sahara. Thème Eau et Environnement: 50-54 p
10. Bouderbala A, Remini B, Hamoudi AS, Pulido-Bosch A (2016b) Assessment of groundwater vulnerability and quality in coastal aquifers: a case study (Tipaza, North Algeria). *Arab J Geosci* 9(3):181
11. Bouderbala A, Remini B, Hamoudi AS, Pulido-Bosch A (2016c) Application of multivariate statistical techniques for characterization of groundwater quality in the coastal aquifer of Nador, Tipaza (Algeria). *Acta Geophys* 64(3):670–693
12. Bouderbala A (2015a) Contribution des méthodes hydrochimiques et géophysiques à l'acquisition de la minéralisation dans les zones côtières cas de la nappe Alluviale de l'oued Nador - Tipaza (Algérie). Thèse de doctorat. Université Hassiba Benbouali de Chlef, p 227
13. Bouderbala A (2015b) Groundwater salinization in semi-arid zones: an example from Nador plain (Tipaza, Algeria). *Environ Earth Sci* 73(9):5479–5496
14. Bouderbala A, Remini B (2014) Geophysical Approach for Assessment of Seawater Intrusion in the Coastal Aquifer of Wadi Nador (Tipaza, Algeria). *Acta Geophysica*, vol. 62, no. 6, Dec. 2014, pp. 1352-1372. DOI: 10.2478/s11600-014-0220-y
15. Boukhelifa M (2014) Contribution à la modélisation de la relation " pluie débit" en absence de données hydrométriques: cas d'une zone urbaine (ville de Tipaza). Mémoires de Magister. 167p
16. Choudhury K, Saha DK, Chakraborty P (2001) Geophysical study for saline water intrusion in a coastal alluvial terrain. *J Appl Geophys* 46:189–200

17. Cocheril H (2019) Dynamique hydrogéologique de flèches littorales: exemple du marais de cap marteau, trois-pistoles, estuaire du saint-laurent. Maîtrise en géographie en vue de l'obtention du grade de maître ès sciences. 132 p
18. Comte JC (2008) Apport de la tomographie électrique à la modélisation des écoulements densitaires dans les aquifères côtiers - Application à trois contextes climatiques contrastés (Canada, Nouvelle Calédonie, Sénégal). Thèse de Doctorat -Académie D'Aix MarseilleUniversité D'Avignon et des Pays de VAUCLUSE / Hydriad, p 202
19. Cooper HH Jr (1959) A hypothesis concerning the dynamic balance of fresh water and salt water in a coastal aquifer. *J Phys Res* 64(4):461–467
20. Demirci I, Gündoğdu NY, Candansayar ME, Soupios P, Vafidis A, Arslan H (2020) Determination and Evaluation of Saltwater Intrusion on Bafra Plain: Joint Interpretation of Geophysical, Hydrogeological and Hydrochemical Data. *Pure appl Geophys* 177(11):5621–5640
21. Inim IJ, Udosen NI, Tijani MN, Affiah UE, George NJ (2020) Time-lapse electrical resistivity investigation of seawater intrusion in coastal aquifer of Ibeno, Southeastern Nigeria. *Appl Water Sci* 10(11):1–12
22. Glangeaud L (1932) Etude géologique de la région littorale de la province d'Alger. Thèse Doctorat Es-Sciences. Paris et Bull. serv. Carte géol. Alger, 2ème série. strat, p 8
23. Glover RE (1959) The pattern of freshwater flow in a coastal aquifer. *J Phys Res* 64(4):439–475
24. Hachemi A (2016) Etude de l'intrusion marine dans les aquifères côtiers. Cas de l'aquifère côtier de l'Oued Nador (W.Tipaza). Thèse de Doctorat en Sciences Agronomiques, Ecole Nationale Supérieure Agronomique (ENSA) – Alger. 194 p
25. Herzberg A (1901) Die Wasserversorgung einiger Noordseebäder. *Journal für Gasbeleuchtung und Wasserversorgung*, München, 44, 815 - 819, 45, 842 - 844
26. Hubbert MK (1940) The theory of groundwater motion. *J Geol* 48(8):785–944
27. Kumar P, Tiwari P, Biswas A, Acharya T (2020) Geophysical and hydrogeological investigation for the saline water invasion in the coastal aquifers of West Bengal, India: a critical insight in the coastal saline clay–sand sediment system. *Environ Monit Assess* 192(9):1–22
28. Kumar VS, Dhakate R, Amarender B, Sankaran S (2016) Application of ERT and GPR for demarcating the saline water intrusion in coastal aquifers of Southern India. *Environ Earth Sci* 75(5):393
29. Huft A (2001) Introduction à la climatologie. De Boeck université. Laval. Canada. 542 p
30. Moulla AS, Guendouz A, Belaidi M, Maamar H, Ouarezki S (2013) Hydrogeochemical and Isotopic Assessment of Seawater Intrusion into wadi Nador Alluvial Aquifer in the Western Algiers Coastal Area (Tipaza, Algeria)
31. Nowroozi AA, Stephen BH, Henderson P (1999) Saltwater intrusion into the fresh water aquifer in the eastern shore of Virginia: a reconnaissance electrical resistivity survey. *J Appl Geophys* 42:1–22
32. Oyeyemi KD, Aizebeokhai AP, Oladunjoye MA (2015) Integrated Geophysical and Geochemical investigations of saline water intrusion in a coastal alluvial terrain, Southwestern Nigeria. *Int J Appl Environ Sci* 10(4):1275–1288
33. Priju CP, Jose NP, Francis J, Balan V, TP SS, Prasad NN (2018) fresh-saline water interface in the shallow coastal aquifers of cherthala-alappuzha coast: application of electrical resistivity techniques. *Hydrology Journal*, Vol. 40& 41, Issue 1–4Jan. –Dec. 2017 & 2018, pp. 16-27
34. Sathish S, Elango L, Rajesh R, Sarma VS (2011) Assessment of seawater mixing in a coastal aquifer by high resolution electrical resistivity tomography. *Int J Environ Sci Technol* 8(3):483–492
35. Geometrics Inc. and, OYO, Inc (2005) Seislmager/2DTM Manual Version 3.1, Pickwin v. 3.14, Plotrefa v. 2.70. OYO Corporation
36. Senthilkumar S, Vinodh K, Babu GJ, Gowtham B, Arulprakasam V (2019) Integrated seawater intrusion study of coastal region of Thiruvallur district, Tamil Nadu, South India. *Appl Water Sci* 9(5):1–20
37. Taibi Y, Hamadache S (1992) Contribution à l'étude hydrogéologique de la basse vallée de l'oued Nador - Tipaza. Mémoire de fin d'études, USTHB, Alger, Algérie. 150 p
38. Thornthwaite CW (1948) An approach toward a rational classification of climate. *Geogr Rev* 38(1):55–94
39. Yusuf MA, Abiye TA (2019) Risks of groundwater pollution in the coastal areas of Lagos, southwestern Nigeria. *Groundw sustainable Dev* 9:100222

Figures

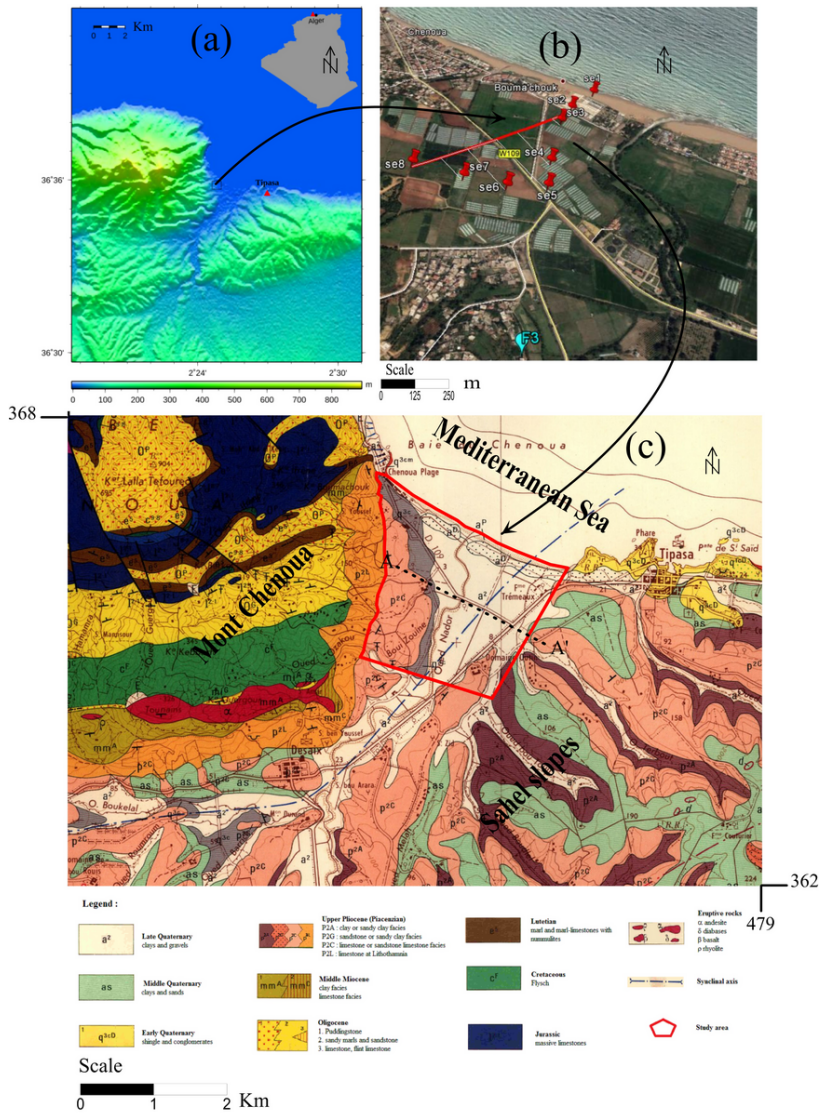


Figure 1

a) Altimetry of the study area. b) Positioning of the electrical soundings and the F3 borehole. c) Geological map of the study area (extracted from the map of the geological service of Algeria (1962)), the frame in red color is the study area and the line A-A' schematic geological section (see Fig. 2).

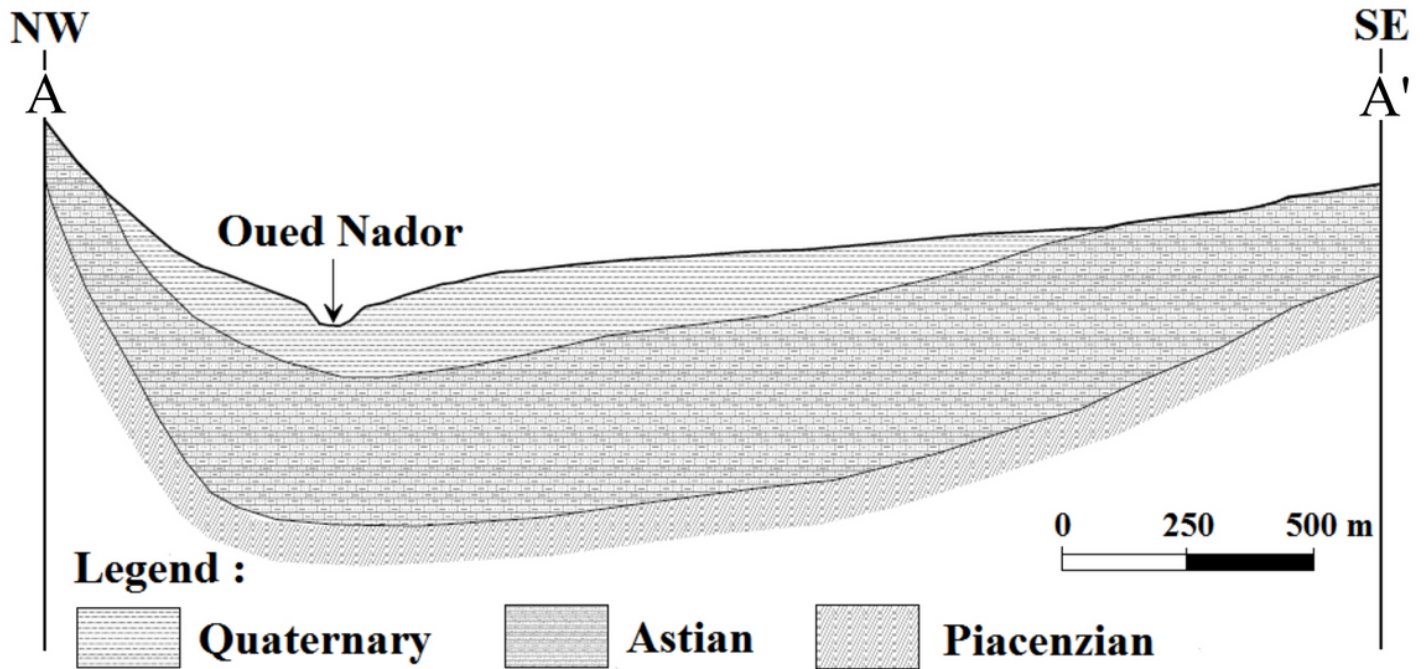


Figure 2

Schematic geological section A-A' (Fig2.) perpendicular to the axis of the syncline (Boderbala, 2015).

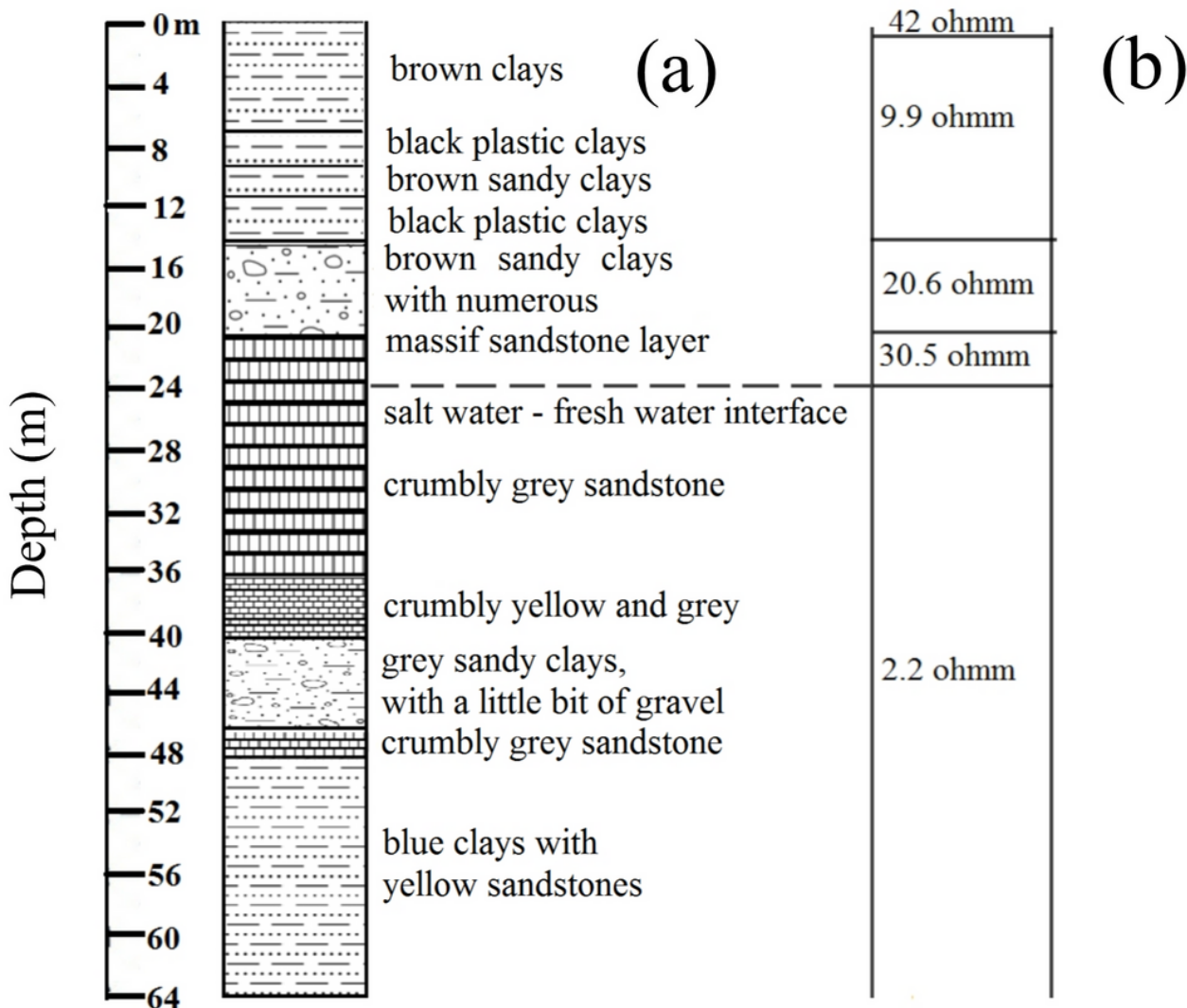


Figure 3

Litho-stratigraphic log of borehole F3 (a) and standard sondage (b) after Taibi and Hamadache (1992).

Rain & Temperature (2017 -2018)

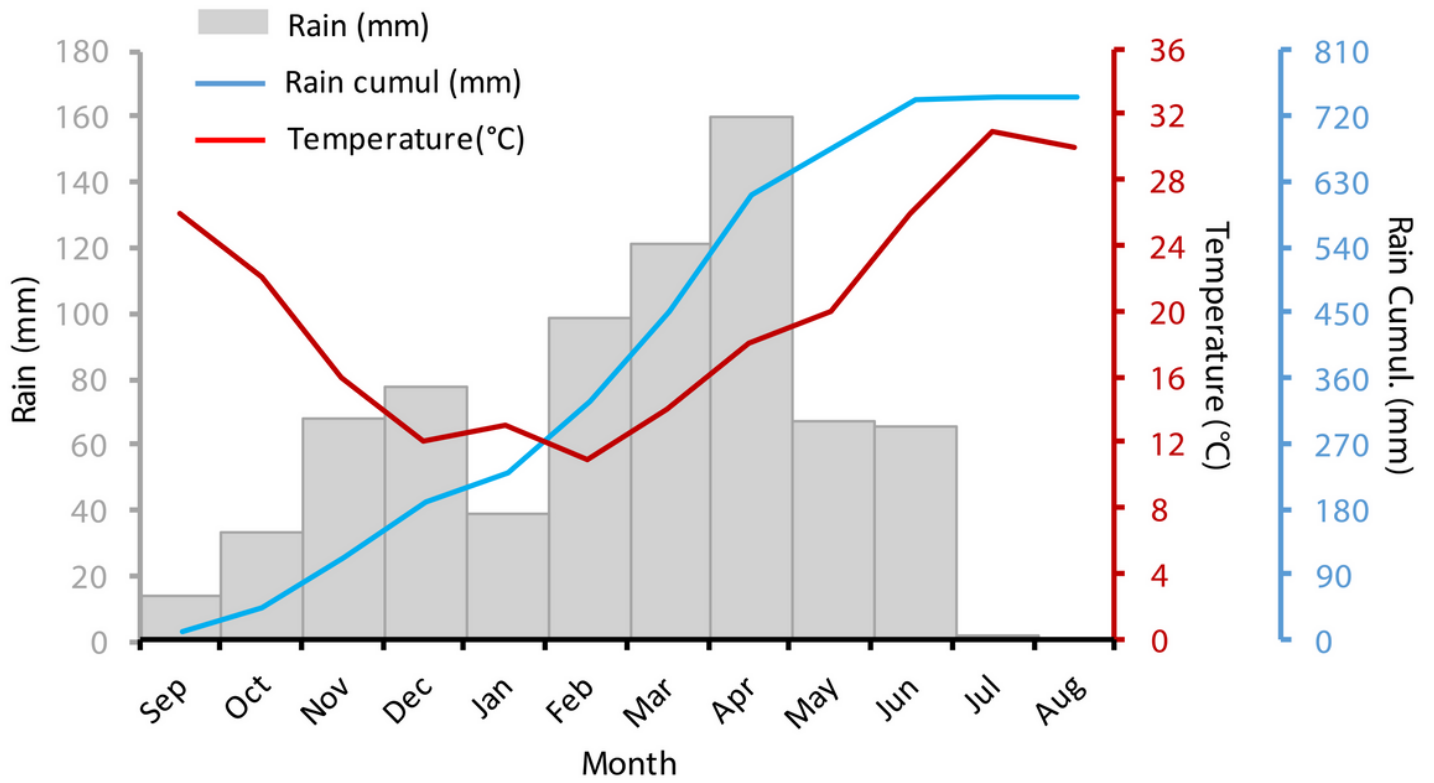


Figure 4

Rainfall- temperature variations between September 2017 and August 2018.

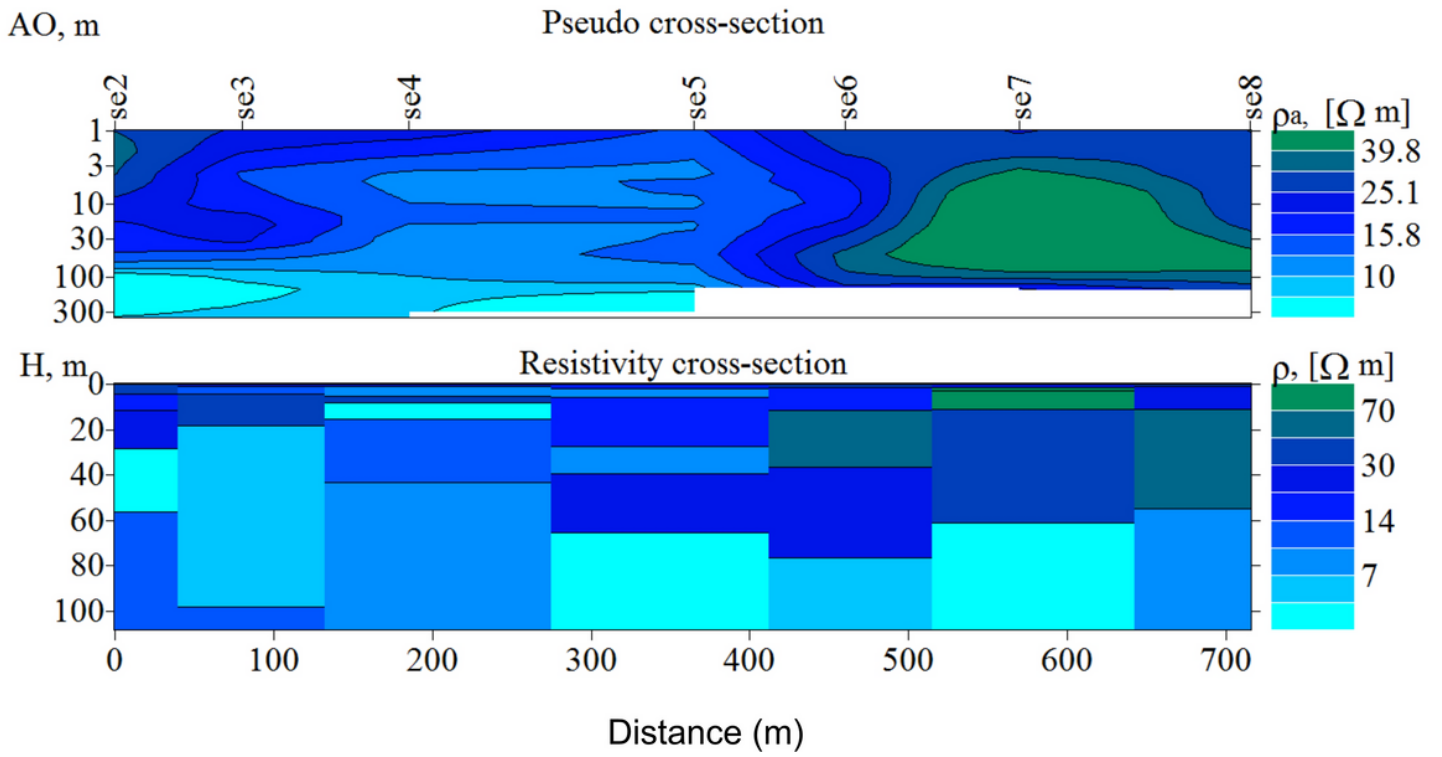


Figure 5

Pseudo-section of the apparent resistivity (a) and the actual values of the geoelectric section (May 2018).

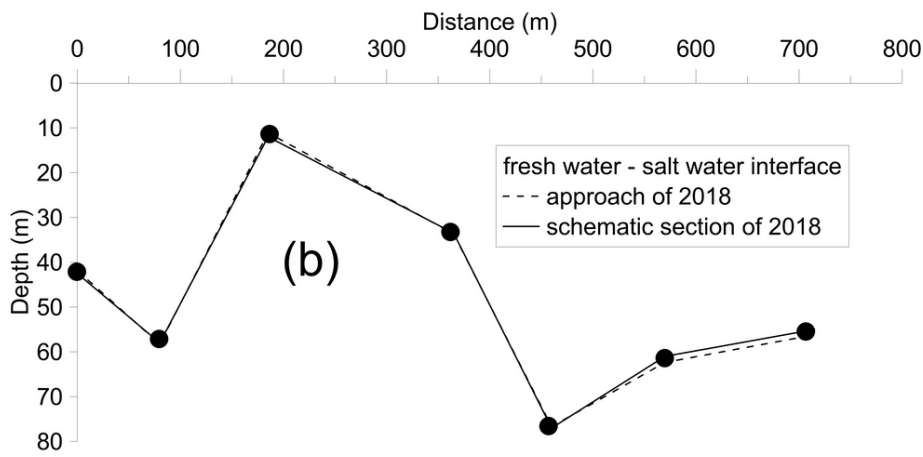
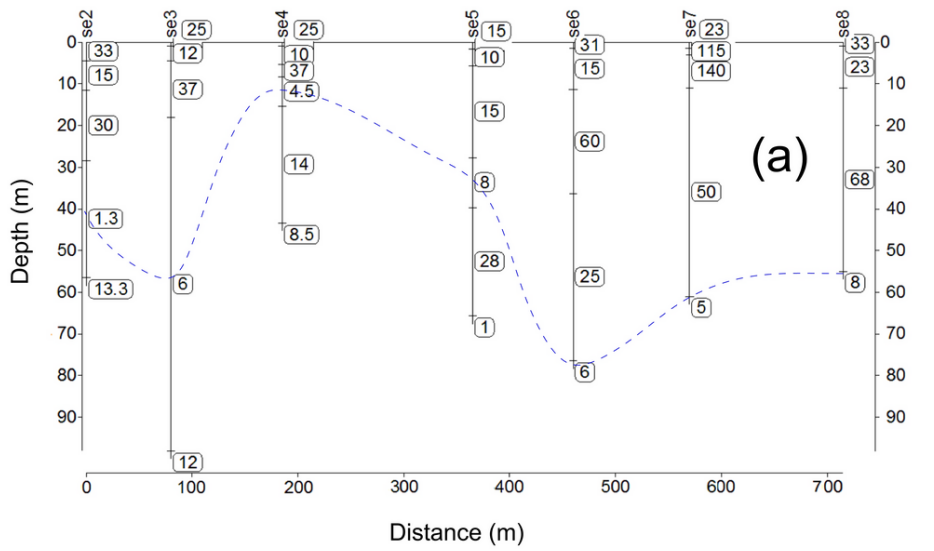


Figure 6
 a) Schematic section representing the freshwater-saltwater interface for May 2018 and b) Comparison between the position of the freshwater-saltwater interface obtained from the Ghyben-Herzberg Hydrostatic Approach Scenario and that obtained from the schematic section released from the results of the May 2018 electrical survey measurement campaign (exaggeration factor vertical scale x 15).

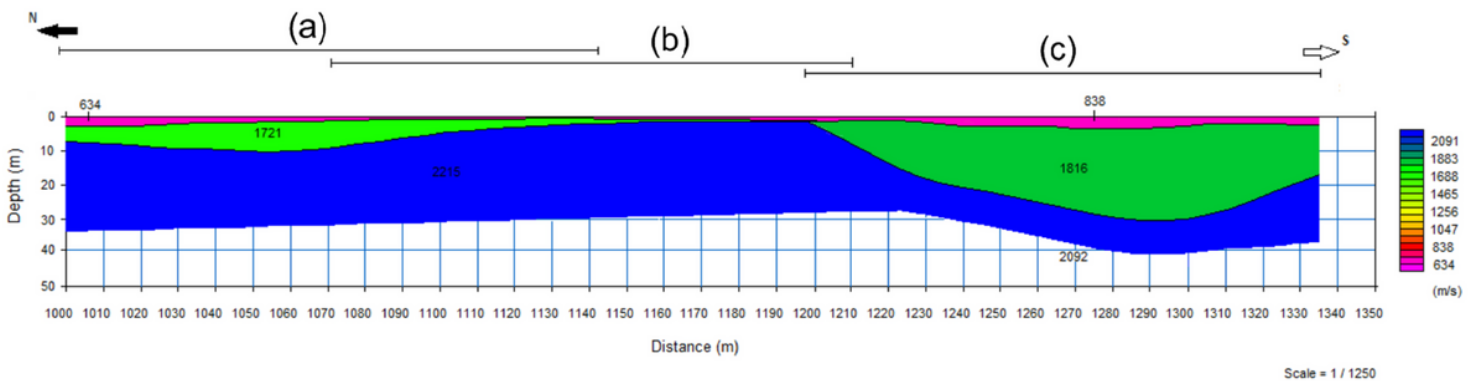


Figure 7
 General geoseismic model of velocity and depth variations.